Ultra-sensitive absorption-based gas detecting using graphene-covered periodic photonic crystal slabs resonating under critical coupling condition at mid-infrared frequencies

Mohammad Mahdi Ghods and Majid Afsahi

***Abstract*—In this paper, a novel chemical sensor is presented based on graphene deposited on the periodic pattern of the photonic crystal. The sensor structure is very simple to fabricate. Also, the proposed sensor thickness in the order of the nanometer makes it compact and suitable for integrating with optical equipment. The principle of sensing is based on the doping process of graphene due to the adsorption of the chemical molecules that serve as charge carriers. The sensor action under critical coupling results in generating the mid-infrared fano-resonance of the half-absorption band. Then, manipulating the graphene Fermi energy and geometrical parameters, a high quality factor can be attained in the resonance frequency that can provide the sensing possibility through the wavelength interrogation method. The results demonstrate that the proposed sensor can detect the chemicals with spectral shifts of $10pm$ for steps of 5 charge carriers which is equal to a resolution smaller than $0.1ppm$. Compared with other types of chemical graphene-based sensors employing optical fibers and plasmonic Fabry-Perot cavity, high resolution and sensitivity as well as the very simple geometry of the proposed sensing structure make it a promising candidate for ultra-sensitive chemical and biochemical detection.**

***Index Terms*—Photonic crystal, Graphene, Critical coupling, Sensor.**

I. Introduction

GRAPHENE has attracted much attention in research scopes of the tunable optical devices[1], [2], [3]. It is an ultra-thin material with a honeycomb pattern that has great properties such as optical transparency, high electron mobility and tunable conductivity[4]. In addition, it can support the plasmonic modes with losses lower than the noble metals such as gold and silver[5], [6]. Most of the potential graphene applications in electronics and photonics are based on its tunable conductivity. It can be controlled electrically and chemically [7]. One of the important graphene capabilities is in realizing optical sensors. Graphene applications in the optical sensing are classified into two types consisted of refractive index sensors and absorption-based sensors. The graphene-based refractive index sensors act based on the plasmonic resonance due to surface plasmon polaritons excitation in the graphene-dielectric boundary as changing the refractive index of the dielectric material can shift the plasmonic resonance wavelength of the sensor, thus detecting analytes based on wavelength interrogation method[8]. This property arranges the action principle of some graphene-based plasmonic sensors such as biochemical sensors using Kretschmann configuration [9], [10], graphene nanoribbons [11] and graphene-based photonic crystal fiber sensors [12], [13], [14].

The absorption-based graphene-covered sensors operate through chemical doping of graphene [15], [16] as chemicals adsorbed by graphene can change the graphene conductivity, thus changing the optical features of the photonic structure[7]. Then, observing the sensor output, it is possible to detect chemical changes of the sensing medium. In recent years, the absorption-based graphene-covered optical sensors have been realized based on the configurations of near-infrared fibers [17], [18], [19], [20] and Fabry-Perot resonators [7], [21]. However, it is still required to develop the sensing parameters such as sensitivity and resolution of these detectors. In addition, it is applicable to realize the ultra-thin and compact structure of these sensors that can simplify the fabrication technology and the integration process with photonic devices. In this paper, an ultra-sensitive graphene-based with high resolution smaller than $1ppm$ is realized to act in the mid-infrared frequencies. The proposed structure is very simple and it consists of a graphene layer deposited on a photonic crystal slab under a periodic pattern. The sensor thickness is equal to 300 nm and it has a planar geometry that can considerably comfort the fabrication and package process. The optical action of the proposed sensing structure is based on resonating under critical coupling condition. In the following, the coupled-mode theory (CMT) is reviewed to describe the sensor electromagnetic operation. Then, the sensor structure is introduced and discussed. Manipulating the bandwidth of the absorption spectrum of the sensor, an ultra-narrow absorption spectrum is attained in order to facilitate the wavelength interrogating in the sensing process. Finally, the sensitivity and the resolution of the proposed graphene-based sensor are obtained that can be compared with other types of sensing structures reported in recent years.

This work was supported by Semnan Univesity. The authors are with the Department of Electrical and Computer Engineering, Semnan University, Semnan, Iran, 1911135131 (e-mail: mahdi.ghods@semnan.ac.ir ; m_afsahi@semnan.ac.ir(corresponding author)).

This is a preliminary version of this paper for an issue of this journal, but has not been fully edited. Content may change prior to final publication. Citation information: DOI 10. Transactions on NanoBioscience

II. Using Coupled Mode Theory to Realize Narrowband Absorption Under Critical Coupling Condition

In a general case, the light absorption spectrum of a single-mode graphene-covered optical resonator with m ports can be expressed by CMT (coupled-mode theory) equation[22], [23]

$$A = \frac{4}{m}\frac{\gamma_a\gamma_r}{(w-w_0)^2+(\gamma_a+\gamma_r)^2} \tag{1}$$

Where w is the angular frequency, w_0 is the resonance angular frequency, γ_r and γ_a are the radiation loss rate and dissipative loss rate respectively and m is the port number. The radiation rate is dependent on the geometrical parameters of the resonator, while the dissipative rate is related to the dispersion due to graphene. From equation. 1, for $\gamma_a = \gamma_r$, namely critical coupling, the maximum value of the absorption A can be given by

$$A_{max} = \frac{1}{m} \tag{2}$$

Therefore, maximum absorption for a two ports resonator under critical coupling condition is equal to 0.5.
On the other hand, the absorption bandwidth is defined with the full width at half maximum (FWHM) and it can be given by:

$$\Gamma_{FWHM} = 2|w_1 - w0| \tag{3}$$

Where w_1 is the half-maximum absorption frequency. Combining equation. 1 and equation. 3, the absorption bandwidth can be concluded

$$\Gamma_{FWHM} = 2(\gamma_a + \gamma_r) \tag{4}$$

Hence, by manipulating the radiation rate and dissipative rate the bandwidth can be tuned.

III. Design and Analysis of the Proposed Structure and Tailoring It for Sensing Based on Wavelength Interrogation Method

The proposed structure unit cell is shown in Fig. 1. It consists of a graphene layer deposited on a periodic photonic crystal slab with periodicity $p = 20\mu m$. The slab clad is silicon material with the refractive index of 3.5 and its hole is made of a silica material with the refractive index of 1.5 and radius of $r = 2\mu m$. The thickness of the structure is equal to 300 nm. The structure is two ports and a normal incident is considered to excite the structure. The lossless photonic crystal slab underneath supports guided resonance with electromagnetic energy strongly confined within the slab, acting as the leaky resonator.

Graphene is modeled as a two dimensional material with the optical surface conductivity of σ_g that is a sum of the interband σ_{inter} and intraband optical transitions σ_{intra} as follow [24]:

$$\sigma_{intra} = i\frac{e^2K_BT}{\pi\hbar^2(w+i\tau^{-1})}\left(\frac{E_f}{K_BT} + 2ln(e^{(-E_f/K_BT)}+1)\right) \tag{5}$$

and

$$\sigma_{inter} = \frac{ie^2E_f}{4\pi\hbar}Ln\left(\frac{2E_f-(w+i\tau^{-1})\hbar}{2E_f+(w+i\tau^{-1})\hbar}\right) \tag{6}$$

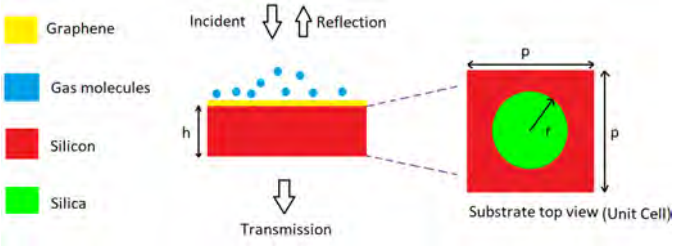

Fig. 1. The proposed structure unit cell schematic view under normal incident excitation. The dimensions of the sensor structure in micrometer are $p = 20$, $h = 0.3$ and $r = 2$. Graphene layer is deposited on a substrate of the periodic photonic crystal pattern.

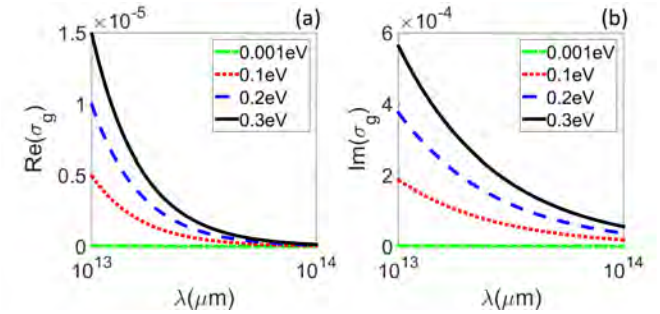

Fig. 2. (a) The real part and (b) the imaginary part of the graphene conductivity are plotted as the functions of frequency for different Fermi energy. It is obvious that the imaginary part is dominant to the real part in the mid-infrared frequencies.

Where $T = 300K$ is the temperature, $\hbar$ is the reduced Planck constant, e is electron charge, E_f is the Fermi energy and $\tau = 0.6\ Ps$ is the carrier relaxation time [5].
According to the previous section analysis, with tuning the dissipative rate and the radiation loss rate, one can obtain a half absorption with narrowband FWHM, thus tailoring the quality factor of the structure to employ in the wavelength interrogation method of the sensing process. The radiation loss γ_r is related to the silica hole radius of r. On the other hand dispersion loss in graphene material can be directly related to the dissipative rate of γ_a.
The real and imaginary parts of the graphene conductivity are plotted in Fig. 2. Obviously, tuning Fermi energy can result in adjusting the conductivity which is related to the energy losses in graphene. So, the dissipative rate γ_a can be controlled by changing the Fermi energy.
In the following, the absorption spectrum of the structure is plotted in Fig. 3 for different values of the Fermi energy and radius of r. The FWHM values of the performed designs in Fig. 3 are listed in Table. 1. As can be seen, the minimum value of FWHM of 5.968 nm is attained for $E_f = 0.2eV$ and $r = 2\mu m$.
In the following, the diffraction spectrum of the proposed structure is plotted in Fig. 4 for Fermi energy of $E_f = 0.2eV$ and radius $r = 2\mu m$. As shown the transmission and the reflection exhibit an asymmetric Fano-shape function while the absorption exposes a symmetric Lorentz-shape function.

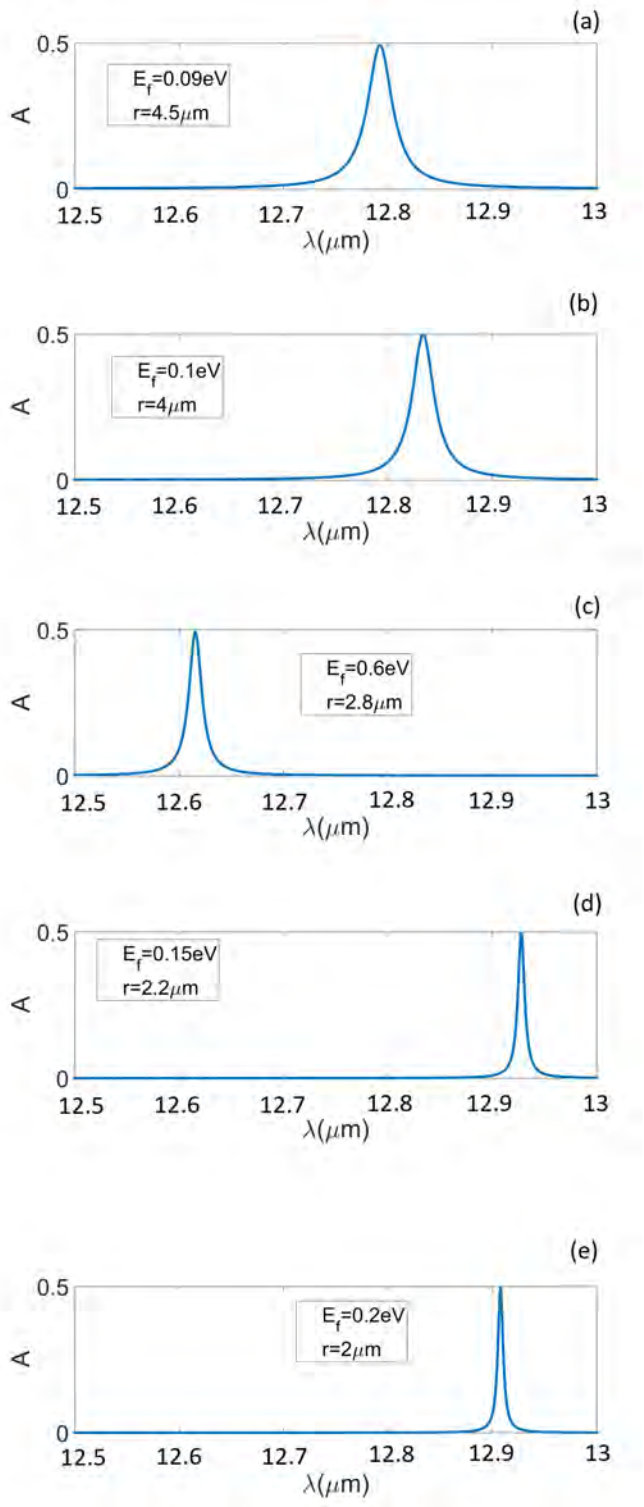

Fig. 3. The absorption spectrum of the proposed structure for different values of the Fermi energy E_f and radius r. Obviously, the highest quality factor can be attained for $E_f = 0.2eV$ and $r = 2\mu m$.

IV. The Sensing Process and the Results

Based on the previous section results, the proposed structure with $E_f = 0.2eV$ and $r = 2\mu m$ is employed as the optimum sensing structure. The sensing process is based on chemical doping of graphene where gas molecules adsorbed on graphene surface change its charge carriers. The graphene surface charge carriers changes result in changing the Fermi energy that can be observed in the resonance frequency shifts of the sensor absorption spectrum. Based on the perturbation theory[25], the spectral shits can be expressed by

$$\triangle w_0 = Im(\sigma_g)\frac{\iint \mid E_{xy} \mid^2 dxdy}{W_0} \tag{7}$$

Where E_{xy} is the electric field in the graphene plane, W_0 is the stored energy in the structure and Im denote the imaginary part of a complex phrase, respectively. It is remarkable that the changes of the Fermi energy are very small (in the order of lower than milielectronvolt) in sensing process. So, the proposed sensor action can conform to perturbation theory. From equation 7, the resonance frequency of the proposed structure is directly dependent on two parts of electric field E_{xy} coupled with graphene and the imaginary part of the graphene conductivity. The normalized electric field coupled with graphene on the X-Y cross-sectional plane is plotted in Fig. 5. It is an even mode. As can be seen, it is maximum in the resonance wavelength which can result in high spectral shift $\triangle w_0$.

The second factor related with $\triangle w_0$ is $Im(\sigma_g)$. On the other hand, the losses in the graphene are related to the real part of the conductivity $Re(\sigma_g)$ and can influence the spectrum amplitude. However, in the mid-infrared frequencies the imaginary part is dominant to the real part. This matter is obvious in Fig. 2 where the imaginary part value of the conductivity is very larger than the real part value of the conductivity from 10 to 100 THz. In other words, in the mid-infrared the spectral resonance shifts are dominant to spectral amplitude changes which can provide the sensing process based on the wavelength interrogation method.

TABLE I
The Parametric Results Obtained from Fig. 3

The number	$E_f(eV)$	$r(\mu m)$	FWHM(nm)
1	0.09	4.5	28.788
2	0.1	4	25.004
3	0.6	2.8	14.61
4	0.15	2.2	7.610
5	0.2	2	5.968

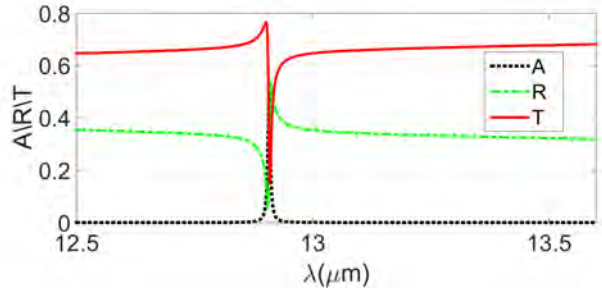

Fig. 4. The diffraction spectrum of the structure. As shown the reflection and transmission spectrum exhibit an asymmetric Fano-shape function while the absorption spectrum shows a symmetric Lorentz-shape function.

The sensitivity can be given by

$$S = \frac{\Delta\lambda_r}{\Delta N_c} \tag{8}$$

Where ΔN_c is the charge carriers number per square micrometer and $\Delta\lambda_r$ is the resonance wavelength shift. In the following, the sensor absorption spectrum is plotted for Fermi energy from 0.2 to $0.225eV$ in Fig. 6. It must be noticed that the proposed sensing structure has a working point. In other words, Fermi energy must be tuned at $0.2eV$ before locating the sensor in the detection environment. Then, the Fermi energy changes as the chemical molecules are adsorbed with graphene. Changing Fermi energy can result in shifting resonance wavelength. This matter is observable in Fig. 6 where the resonance wavelength moves to the lower wavelength.

The relation between the charge carriers number N_c and Fermi energy E_f can be given by [7]

$$N_c = \frac{E_f^2}{\pi(\hbar v_f)^2} \tag{9}$$

Where $v_f = 1.1 \times 10^6 m/s$ is the Fermi velocity in graphene. Using equation. 9, the resonance wavelength shift is plotted per charge carriers number N_c in Fig. 7. As can be seen, it almost follows from a linear function from 2.435×10^4 to 3.082×10^4 per square micrometer of N_c. To calculate the resolution of the proposed sensing structure, a spectral shift of 10 pm is considered which is simple to measure based on realistic value $\Delta\lambda_{instr} = 1pm$ according to the OSA instrumental resolution in the experimental setup [26]. This spectral shift is according to charge carriers changes equal to 5 electrons or holes per square micrometer as shown in Fig. 7. This value is equal to resolution of around 0.1 ppm gas concentration [15]. In other words, the proposed sensor can detect chemicals adsorbed on graphene surface with steps of 5 charge carriers per square micrometer with resonance wavelength shifts of 10 pm. So the resolution of the proposed sensing structure is equal to 5 charge carriers per square micrometer. Using equation. 9, this value exhibits the Fermi energy change of $20\mu eV$. To better understand the sensing process the absorption spectrum is plotted for changes of $\Delta E_f = 20\mu eV$ in Fig. 8. As shown these changes of the Fermi energy result in shifting the resonance wavelength of 10 pm.

The Fano-shape transmission spectrum of the sensor is depicted in Fig. 10 for detection steps of 150 charge carries that is equal to 1 ppm [7], approximately. As shown, the sensor can detect chemical doping of graphene with steps of 1 ppm gas molecules concentration through spectral shifts by around 300 pm in the transmission spectrum.

V. Discussion and Comparison

As mentioned, the operation of the proposed sensor is based on doping graphene. Actually, every chemical molecule interacting with graphene changes graphene surface charge carriers. The relation between the chemical molecules number of N and the charge carriers number N_c can be given by the following equation

$$N = \frac{N_c}{\beta} \tag{10}$$

This relation explains that every chemical or biochemical molecule adsorbed by graphene can change the charge carriers N_c with coefficient of $1/\beta$. β has been given for some chemical gases such as NO_2, NH_3 and H_2O [16]. These values of β are around 0.1, 0.027 and 0.025 for NO_2, NH_3 and H_2O, respectively. Using equation. 10, in each sensing step, the proposed sensor enables detecting of 50, 185 and 200 molecules of gases NO_2, NH_3 and H_2O, respectively. This calculation can be performed for other types of the chemicals or biochemicals if the coefficient of β is available.

The proposed detecting structure can be compared with other types of graphene-based chemical sensors reported in recent years. This comparison is demonstrated in Table. 2. As can be seen, the proposed sensor with thinner thickness as well as higher resolution has a better action for fabrication and detection.

In recent years, other groups of the chemical graphene-covered sensors have been presented that operate based on optical fibers [17], [18], [19], [20]. Their resolution is on the order of 0.1 ppm that equalizes with the proposed sensor. However, the fabrication process of them is more difficult than the proposed sensing structure.

As mentioned, the proposed sensing structure has working point with a value of $E_f = 0.2eV$ as before placing the sensor in the sensing medium, the graphene Fermi energy must be tuned at this value. This can be performed through a primary chemical doping as used in reference [27]. Hence, the value of charge carriers N_c can be calculated by considering the surface area of the proposed structure. For example, the proposed sensor with 20 unit cells needs a chemical doping with a charge carrier number of 19.48×10^7 electrons or hols.

In our work, The ability to manipulate the absorption bandwidth enables realizing of a wide range of applications such as lasing emission [28], color filtering, switching [29], [30], light modulation [31], photodetection, and energy harvesting [32], [33].

The proposed structure can be influenced by the factors such as molecular Interference, electromagnetic interference, optical radiation and temperature, thus producing sensing errors in the results. Molecular Interference may impress the proposed sensor if the environment consisting of the desired gas is perturbed with other types of gases or chemicals. Nevertheless, many molecules have active vibrational bands at terahertz to mid-infrared frequencies [34]. The coupling modes of these molecules with the proposed sensor resonances can generate characteristic dips in the reflection spectra because of the absorption. Detecting the location of these dips, it is feasible to specify the molecule type. The changes in the optical radiation can influence the proposed optical sensor. Optical sensors utilizing modulated light and selective detecting systems are not sensitive to changes in these radiations [35].

Electromagnetic interference is unwanted noise or interference in an electrical path or circuit (in an optoelectronic device) caused by an outside source. It can impress the results of the proposed sensing structure. However, the proposed optical sensors with optical detection are insensitivity on the electromagnetic interference [7].

The proposed graphene-based sensing structure can be utilized

TABLE II
COMPARISON WITH OTHER TYPES OF GRAPHENE-BASED CHEMICAL SENSORS

Ref.	Type	Resolution	Thickness	The frequency band
[7]	Plasmonic resonator	150 μm^{-2}	25 μm	Far-infrared
[21]	Dielectric grating	100 μm^{-2}	18.9 μm	Far-infrared
This work	Dielectric grating	5 μm^{-2}	300 nm	Mid-infrared

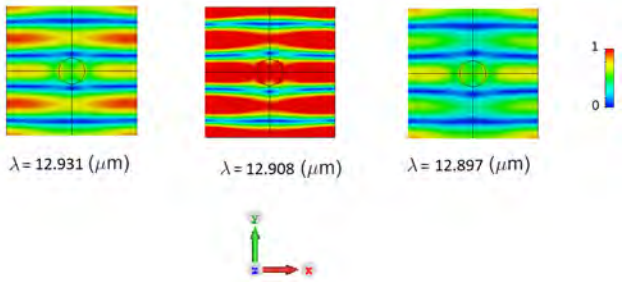

Fig. 5. The normalized electric field distribution in the graphene location. As shown, the maximum rate of the electric field is coupled with graphene in resonance wavelength $\lambda_r = 12.908\mu m$.

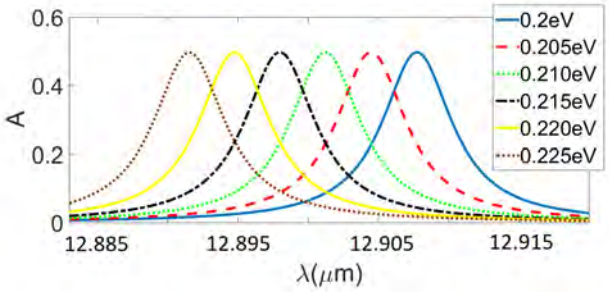

Fig. 6. The absorption for different Fermi energy from 0.2eV to 0.225eV.

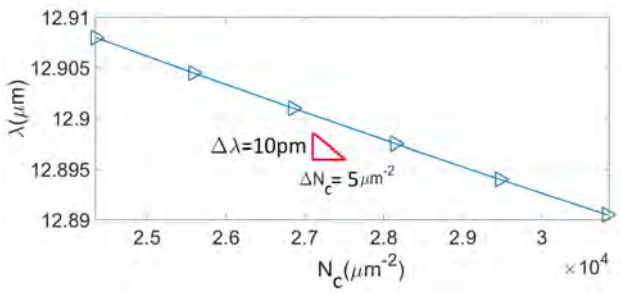

Fig. 7. The resonance wavelength shifts as a function of charge carriers N_c per square micrometer.

to detect many diverse chemicals such as gas molecules[15], [16], biomolecules [36], [37], metals, polymers and organic molecules[38], [39].

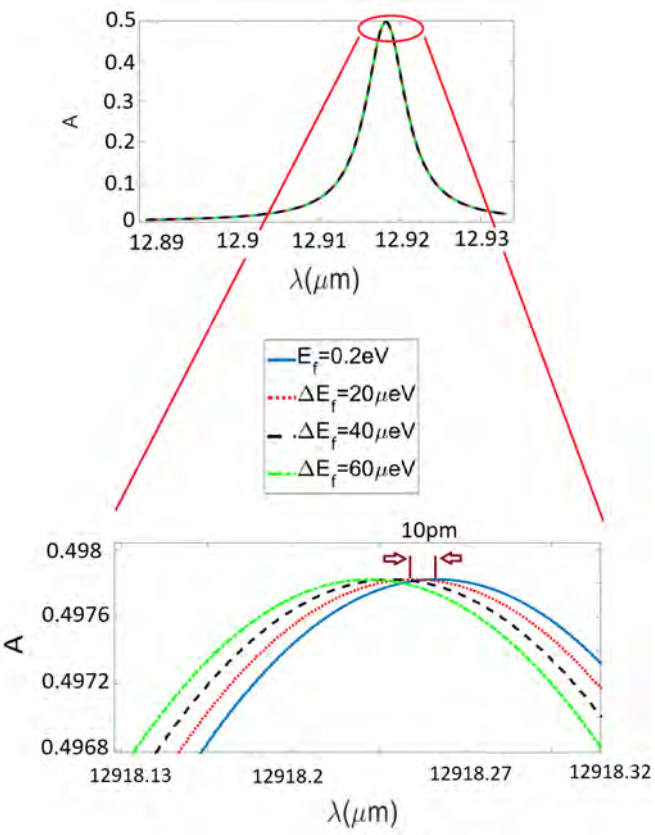

Fig. 8. The spectral shifts of sensor absorption spectrum with value of $10pm$ for changes of $20\mu eV$.

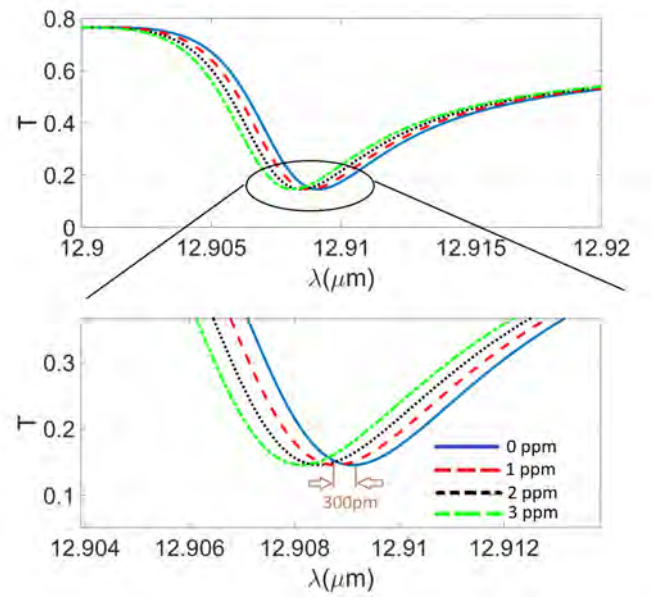

Fig. 9. The transmission spectrum of the proposed sensor for chemical doping changes of $1ppm$.

VI. CONCLUSION

The graphene-covered periodic photonic crystal structure is presented for chemical sensing in the mid-infrared frequency range. The sensor acts based on chemical doping of

graphene because of its Fermi energy changes due to chemical molecules served as charge carriers acceptors or donors. The sensor has a sharp absorption spectrum under critical coupling resonance. The strong electric field coupled with graphene in the resonance frequency can increase the spectral shifts in the wavelength interrogation process. The results demonstrate that the attained resolution with a value of 5 charge carriers per square micrometer is smaller than other types of the graphene-based sensors presented in recent years. Compared with chemical graphene-covered sensors utilizing optical fibers that have a difficult fabrication process, the proposed structure has a planar geometry and its fabrication is simple. Also, the very thin thickness of the proposed sensor makes it a promising candidate to use in compact optical devices for chemical or biochemical detection.

VII. ACKNOWLEDGEMENT

This work is supported by semnan university.

REFERENCES

[1] N. I. Zheludev and Y. S. Kivshar, "From metamaterials to metadevices," Nature Materials, vol. 11, no. 11, pp. 917–924, 2012.

[2] S. Xiao, T. Wang, T. Liu, C. Zhou, X. Jiang and J. Zhang, " Active metamaterials and metadevices: A review," J. Phys. D: Appl. Phys., vol. 53, p. 503002, 2020.

[3] Q. Xu, Y. Lu, J. Yuan, Y. Zhang, and Q. Bao, "Graphene Plasmonics," Graphene Photonics, Optoelectronics, and Plasmonics, pp. 101–130, 2017.

[4] O. M. Daraei, K. Goudarzi, and M. Bemani, "A tunable ultra-broadband terahertz absorber based on two layers of graphene ribbons," Opt. Laser Technol., vol. 122, p. 105853, 2020.

[5] S. E. Hosseininejad and N. Komjani, "Waveguide-Fed Tunable Terahertz Antenna Based on Hybrid Graphene-Metal Structure," IEEE Transactions on Antennas and Propagation, vol. 64, no. 9, pp. 3787–3793, 2016.

[6] J. Guo, L. Wu, X. Dai, Y. Xiang, and D. Fan, "Absorption enhancement and total absorption in a graphene-waveguide hybrid structure," AIP Advances, vol. 7, no. 2, p. 025101, 2017.

[7] B. Vasić and R. Gajić, "Graphene-Covered Photonic Structures for Optical Chemical Sensing," Physical Review Applied, vol. 4, no. 2, p. 024007, 2015.

[8] P. Yari, H. Farmani, and A. Farmani, "Steering of Guided Light with Graphene Metasurface for Refractive Index Sensing with High Figure of Merits," Plasmonics, 2021.

[9] P. S. Menon, N. A. Jamil, G. S. Mei, A. R. M. Zain, D. W. Hewak, C.-C. Huang, M. A. Mohamed, B. Y. Majlis, R. K. Mishra, S. Raghavan, and N. Bhat, " Multilayer CVD-graphene and MoS_2 Ethanol Sensing and Characterization Using Kretschmann-Based SPR," IEEE Journal of the Electron Devices Society, vol. 8, pp. 1227-1235, 2020.

[10] M. B. Hossain, T. Tasnim, L. F. Abdulrazak, M. M. Rana, and M. R. Islam, "A Numerical Approach to Design the Kretschmann Configuration Based Refractive Index Graphene-MoS_2 Hybrid Layers With $TiO_2 - SiO_2$ Nano for Formalin Detection," Photonic Sensors, vol. 10, no. 2, pp. 134–146, 2019.

[11] S. Luo, X. Chen, Y. He, Y. Gu, C. Zhu, G.-H. Yang, and L.-L. Qu, "Recent advances in graphene nanoribbons for biosensing and biomedicine," Journal of Materials Chemistry B, 2021.

[12] H. Yang, M. Liu, Y. Chen, L. Guo, G. Xiao, H. Liu, J. Li, and L. Yuan, "Highly Sensitive Graphene-Au Coated Plasmon Resonance PCF Sensor," Sensors, vol. 21, no. 3, p. 818, 2021.

[13] Y. E. Monfared and M. Qasymeh, "Plasmonic Biosensor for Low-Index Liquid Analyte Detection Using Graphene-Assisted Photonic Crystal Fiber," Plasmonics, vol. 16, no. 3, pp. 881–889, 2021.

[14] J. Tian, C. Xu, S. Cui, L. Ma, and Y. Fu, "A Photonic Crystal Fiber-Based Biosensor with Quasi-D-shaped Layout and ITO-Graphene Combination," Plasmonics, vol. 16, no. 5, pp. 1451–1460, 2021.

[15] F. Schedin, A. K. Geim, S. V. Morozov, E. W. Hill, P. Blake, M. I. Katsnelson, and K. S. Novoselov, "Detection of individual gas molecules adsorbed on graphene," Nature Materials, vol. 6, no. 9, pp. 652–655, 2007.

[16] O. Leenaerts, B. Partoens, and F. M. Peeters, "Adsorption of H2O, NH3, CO, NO2, and NO on graphene: A first-principles study," Physical Review B, vol. 77, no. 12, p. 125416, 2008.

[17] B. C. Yao, Y. Wu, A. Q. Zhang, Y. J. Rao, Z. G. Wang, Y. Cheng, Y. Gong, W. L. Zhang, Y. F. Chen, and K. S. Chiang, "Graphene enhanced evanescent field in microfiber multimode interferometer for highly sensitive gas sensing," Optics Express, vol. 22, no. 23, p. 28154, 2014.

[18] Y. Wu, B. Yao, A. Zhang, Y. Rao, Z. Wang, Y. Cheng, Y. Gong, W. Zhang, Y. Chen, and K. S. Chiang, "Graphene-coated microfiber Bragg grating for high-sensitivity gas sensing," Optics Letters, vol. 39, no. 5, p. 1235, 2014.

[19] B. C. Yao, Y. Wu, D. J. Webb, J. H. Zhou, Y. J. Rao, A. Pospori, C. B. Yu, Y. Gong, Y. F. Chen, and Z. G. Wang, "Graphene-Based D-Shaped Polymer FBG for Highly Sensitive Erythrocyte Detection," IEEE Photonics Technology Letters, vol. 27, no. 22, pp. 2399–2402, 2015.

[20] T. Hao and K. S. Chiang, "Graphene-Based Ammonia-Gas Sensor Using In-Fiber Mach-Zehnder Interferometer," IEEE Photonics Technology Letters, vol. 29, no. 23, pp. 2035–2038, 2017.

[21] M. M. Ghods and P. Rezaei, "Graphene-Based Fabry-Perot Resonator for Chemical Sensing Applications at Mid-Infrared Frequencies," IEEE Photonics Technology Letters, vol. 30, no. 22, pp. 1917–1920, 2018.

[22] S. Xiao, T. Liu, X. Wang, X. Liu, and C. Zhou, "Tailoring the absorption bandwidth of graphene at critical coupling," Physical Review B, vol. 102, no. 8, p. 085410, 2020.

[23] J. Wang, A. Chen, Y. Zhang, J. Zeng, Y. Zhang, X. Liu, L. Shi, and J. Zi, "Manipulating bandwidth of light absorption at critical coupling: An example of graphene integrated with dielectric photonic structure," Physical Review B, vol. 100, no. 7, p. 075407, 2019.

[24] G. W. Hanson, "Dyadic Green's Functions for an Anisotropic, Non-Local Model of Biased Graphene,"IEEE Transactions on Antennas and Propagation, vol. 56, no. 3, pp. 747–757, 2008.

[25] S. H. Mousavi, I. Kholmanov, K. B. Alici, D. Purtseladze, N. Arju, K. Tatar, D. Y. Fozdar, J. W. Suk, Y. Hao, A. B. Khanikaev, R. S. Ruoff, and G. Shvets, "Inductive Tuning of Fano-Resonant Metasurfaces Using Plasmonic Response of Graphene in the Mid-Infrared," Nano Letters, vol. 13, no. 3, pp. 1111–1117, 2013.

[26] B. Yao, Y. Wu, Y. Cheng, A. Zhang, Y. Gong, Y.-J. Rao, Z. Wang, and Y. Chen, "All-optical Mach–Zehnder interferometric NH3 gas sensor based on graphene/microfiber hybrid waveguide," Sensors and Actuators B: Chemical, vol. 194, pp. 142–148, 2014.

[27] Y. Yao, M. A. Kats, P. Genevet, N. Yu, Y. Song, J. Kong, and F. Capasso, "Broad Electrical Tuning of Graphene-Loaded Plasmonic Antennas," Nano Letters, vol. 13, no. 3, pp. 1257–1264, 2013.

[28] J. Wang, D. Han, A. Chen, Y. Dai, M. Zhou, X. Hu, Z. Yu, X. Liu, L. Shi, and J. Zi, "Using active gain to maximize light absorption," Physical Review B, vol. 96, no. 19, 2017.

[29] C. Valagiannopoulos, "Controlling Reflection and Transmission with a Single Layer," IEEE Antennas and Propagation Magazine, vol. 57, no. 2, pp. 318–323, 2015.

[30] A. N. Papadimopoulos, N. V. Kantartzis, N. L. Tsitsas, and C. A. Valagiannopoulos, "Wide-angle absorption of visible light from simple bilayers," Applied Optics, vol. 56, no. 35, p. 9779, 2017.

[31] P. Cencillo-Abad, N. I. Zheludev, and E. Plum, "Metadevice for intensity modulation with sub-wavelength spatial resolution," Scientific Reports, vol. 6, no. 1, 2016.

[32] M. H. Elshorbagy, E. López-Fraguas, J. M. Sánchez-Pena, B. García-Cámara, and R. Vergaz, "Boosting ultrathin aSi-H solar cells absorption through a nanoparticle cross-packed metasurface," Solar Energy, vol. 202, pp. 10–16, 2020.

[33] J. Li, X. Chen, Z. Yi, H. Yang, Y. Tang, Y. Yi, W. Yao, J. Wang, and Y. Yi, "Broadband solar energy absorber based on monolayer molybdenum disulfide using tungsten elliptical arrays," Materials Today Energy, vol. 16, p. 100390, 2020.

[34] A. I. McIntosh, B. Yang, S. M. Goldup, M. Watkinson and R. S. Donnan, " Terahertz spectroscopy: A powerful new tool for the chemical sciences?," Chem. Soc. Rev. vol. 41, pp. 2072-2082, 2012.

[35] A. Dybko, " Errors in Chemical Sensor Measurements," Sensors, vol. 1, no. 1, pp. 29-37, 2001.

[36] M. Chen, H. Su, L. Mao, M. Guo, and J. Tang, "Highly sensitive electrochemical DNA sensor based on the use of three-dimensional nitrogen-doped graphene," Microchimica Acta, vol. 185, no. 51, 2017.

[37] R. V. Nair, P. R. Chandran, A. P. Mohamed, and S. Pillai, "Sulphur-doped graphene quantum dot based fluorescent turn-on aptasensor for selective and ultrasensitive detection of omethoate," Analytica Chimica Acta, vol. 1181, p. 338893, 2021.

[38] X. Wang, J.-B. Xu, W. Xie, and J. Du, "Quantitative Analysis of Graphene Doping by Organic Molecular Charge Transfer," The Journal of Physical Chemistry C, vol. 115, no. 15, pp. 7596–7602, 2011.
[39] P. K. Srivastava, P. Yadav, V. Rani, and S. Ghosh, "Controlled Doping in Graphene Monolayers by Trapping Organic Molecules at the Graphene–Substrate Interface," ACS Appl. Mater. Interfaces, vol. 9, no. 6, pp. 5375–5381, 2017.

Mohammad Mahdi Ghods received the B. Sc and M. S. degree in the electrical and computer engineering degree from Semnan University, Semnan, Iran, in 2014 and 2018, respectively. Currently, he is pursuing his PhD with Semnan University. Current research interests include contribution to the study of photonic absorbers, optical modulation, graphene-based optical sensors, and plasmonic nanostructures.

Majid Afsahi received the B.Sc. degree in electrical and electronics engineering from Tehran University, Iran, in 1991, the M.S. degree in electrical engineering from Amirkabir University of Technology in 1993, and the Ph.D degree in electrical and electronics engineering Iran University of Science and Technology, Iran, in 2010. He has taught and done research at Shahid Bahonar University of Kerman on Antennas and RF/Microwave passive structures and he has worked in Telecommunication Company of Iran on cellular and RF systems. In 2010, he joined the Department of Electrical and Computer Engineering, Semnan University Semnan, Iran, as an Assistant Professor. His research interests are in the area of periodic structures, metamaterial media, Antenna and RF passive components in Microwave/THz frequency.